Synthesis and characterization of nickel-group bis(dithiocroconate) complexes and dicyanomethylene-substituted analogues †

William B. Heuer * and Wayne H. Pearson

Chemistry Department, Stop 9B, United States Naval Academy, 572 Holloway Road, Annapolis, MD 21402-5026, USA

Two series of nickel-group metal bis(dithiolene) complexes with ligands 4,5-disulfanylcyclopent-4-ene-1,2,3-trionate (L^1) and 2-dicyanomethylene-4,5-disulfanylcyclopent-4-ene-1,3-dionate (L^2) have been prepared and characterized: $[NBu^n_4]_2[M(L^i)_2]$ (M = Ni, Pd or Pt; i = 1 or 2). Oxidation of the dianion complexes yielded paramagnetic monoanions with ESR spectra indicative of a delocalized b_{3g} HOMO (highest occupied molecular orbital), like that previously found for comparable bis(dithiolene) complexes. The intense low-energy visible absorptions and multiple, reversible reductions exhibited by the dianions likewise suggest that the LUMO (lowest unoccupied molecular orbital) is a ligand-based $a_u(\pi^*)$ orbital, rather than the $b_{1g}(d_{xy})$ orbital as commonly found for such complexes. The stabilization of the ligand-based LUMO in this case is attributed to the strongly electron-withdrawing character of the ligand substituents. Iodination of $[NBu^n_4]_2[Pd(L^2)_2]$ in CH_2Cl_2 solution yielded the novel iodine inclusion compound $[NBu^n_4]_2[Pd(L^2)_2]\cdot I_2$, which crystallizes in space group $P\bar{1}$ with Z = 1, a = 10.792(3), b = 13.995(5), c = 10.737(3) Å, α = 105.48(1), β = 115.15(1) and γ = 76.51(2)° at 25 °C. The I_2 molecules are associated with the complex anions through short [3.1696(9) Å] S · · · I contacts; however, the observed I–I distance [2.7354(4) Å] indicates that the degree of charge transfer associated with this interaction is small.

Planar metal complexes with chelating ethylene-1,2-dithiolato-ligands [metal bis(dithiolenes)] have attracted considerable interest owing to their delocalized electronic structures and rich redox chemistry.[1] Nickel-group metal bis(dithiolene) complexes have found widespread application as components of conducting and magnetic charge-transfer salts[2] and have also proven useful as Q-switch dyes for IR lasers.[3] Accordingly, we have been investigating the co-ordination chemistry of the 4,5-disulfanylcyclopent-4-ene-1,2,3-trionate ion[4] (L^1), which is a sulfur-substituted analogue of the aromatic croconate ($C_5O_5^{2-}$) ion.[5] While several metal–croconate complexes have been described,[6] the co-ordination chemistry of the dithiocroconate analogue L^1 has received little attention up to now.[7] We anticipated that the polar peripheral substituents of metal–dithiocroconate complexes might promote strong intermolecular interactions in the solid state, yielding salts with interesting co-operative electronic and/or magnetic properties. It was also of interest to prepare complexes of the analogous dicyanomethylene-substituted dianion[8] (L^2) in order to explore the influence of the ligand substituents upon the optical and electrochemical properties of the complexes.

This contribution describes the preparation and characterization of two series of symmetrical, dianionic nickel-group bis(dithiolene) complexes containing ligands L^1 and L^2, respectively. Both sets of complexes exhibit unusually intense low-energy visible absorptions and facile reductive electrochemistry. Results of comparative studies of these two series of complexes are presented which provide insight into the electronic structure of the complexes and the origin of their novel spectroscopic and electrochemical properties. The crystal structure of the novel iodine inclusion compound $[NBu^n_4]_2[Pd(L^2)_2]\cdot I_2$ also is reported.

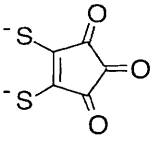

L^1

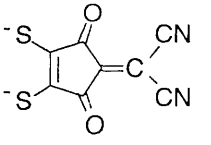

L^2

Experimental

Materials

Dipotassium dithiocroconate (K_2L^1) was prepared as previously described[7a] and gave satisfactory spectra and elemental analysis. Acetonitrile used for electrochemical measurements was spectrophotometric grade (Burdick and Jackson) and was passed down a column of activated Al_2O_3 immediately prior to use. Dichloromethane was refluxed over P_2O_5 and distilled under Ar immediately prior to use. Tetrabutylammonium tetrafluoroborate (Sachem, Inc.) was dried *in vacuo* at 80 °C prior to use. All other reagents were obtained from commercial sources and used without further purification. Elemental analyses were performed by Galbraith Laboratories, Knoxville, TN and Desert Analytics, Tucson, AZ.

Instrumentation

The NMR spectra were run on a General Electric QE-300 FT-NMR system, IR spectra using a Perkin-Elmer System 2000 FTIR spectrometer, UV/VIS spectra using a Hewlett-Packard model 8452A diode-array spectrophotometer, and near-IR measurements using a Galaxy 5040 spectrometer equipped with a quartz beamsplitter and silicon detector. The ESR spectra were recorded on a Bruker ECS-106/9 spectrometer equipped with a Hewlett-Packard model HP5350B frequency counter; field calibration was checked with diphenylpicrylhydrazyl (g = 2.0036). The samples were prepared by low-temperature (MeCN, −20 °C; CH_2Cl_2, −78 °C) electrolysis of argon-saturated solutions containing *ca.* 5×10^{-3} mol dm^{-3} electroactive complex and 0.1 mol dm^{-3} $(NBu^n_4)BF_4$ supporting electrolyte in a fritted H-cell equipped with 4 × 20 mm platinum-flag electrodes. A constant current of 0.4 mA was

† *Non-SI unit employed:* G = 10^{-4} T.

applied for *ca.* 1 h using a PAR model 362 potentiostat, after which a small portion of the solution was transferred under Ar into an ESR tube and immediately frozen in liquid nitrogen. Cyclic voltammetry was performed using a BAS CV-1B potentiostat, Houston Instruments recorder and Fluke digital multimeter. Potentials were measured relative to a silver wire and referenced to an internal ferrocene standard.[9]

Preparation of dithiocroconate complexes

$[NBu^n_4]_2[Ni(L^1)_2]$ 1. A suspension of K_2L^1 (0.20 g, 0.80 mmol) in dimethylformamide (dmf)–water (3:1 v/v, 20 cm^3) was heated to 70 °C and stirred until all solids were dissolved. To this solution was added $NiCl_2·6H_2O$ (0.095 g, 0.40 mmol) dissolved in dmf (3 cm^3). The resulting deep green solution was stirred at 70 °C for 15 min, then filtered into a solution of NBu^n_4Br (0.40 g, 1.2 mmol) in EtOH (5 cm^3). After addition of water (50 cm^3) to ensure complete precipitation, the crude product was collected by vacuum filtration and dried in air. Recrystallization from Pr^iOH–acetone solution yielded black needles with purple reflex (0.30 g, 84%), m.p. 183–184 °C (Found: C, 57.0; H, 8.3; N, 3.1; S, 15.5. $C_{42}H_{72}N_2NiO_6S_4$ requires C, 56.8; H, 8.2; N, 3.2; S, 14.4%).

$[NBu^n_4]_2[Pd(L^1)_2]$ 2. The salt K_2L^1 (0.40 g, 1.6 mmol) was dissolved in water (5 cm^3), and then dmf (30 cm^3) was added. To this solution was added K_2PdCl_4 (0.26 g, 0.80 mmol) dissolved in water (5 cm^3), and the resulting mixture was stirred at 70 °C for 30 min. The deep purple solution was then filtered into a solution of NBu^n_4Br (0.70 g, 1.9 mmol) in water (10 cm^3). Precipitation was completed by addition of water (50 cm^3) and cooling to 5 °C. The solid was collected by vacuum filtration, washed with several small portions of water, and dried in air. Recrystallization from Pr^iOH–acetone yielded maroon needles (0.62 g, 83%), m.p. 193–194 °C (Found: C, 53.7; H, 7.6; N, 3.1; S, 13.5. $C_{42}H_{72}N_2O_6PdS_4$ requires C, 53.9; H, 7.8; N, 3.0; S, 13.9%).

$[NBu^n_4]_2[Pt(L^1)_2]$ 3. The salt K_2PtCl_4 (0.33 g, 0.80 mmol) was dissolved in water (5 cm^3). To this solution was added K_2L^1 (0.40 g, 1.6 mmol) in water (20 cm^3), and the resulting mixture was maintained at 60 °C with stirring for 2 h. The reaction mixture was then cooled to 25 °C and the insoluble $K_2[Pt(L^1)_2]$ was isolated by vacuum filtration, washed first with water then MeOH, and briefly dried in air. The purple powder was redissolved with stirring in warm (60 °C) dmf (10 cm^3), and the resulting deep blue solution was filtered into a solution of NBu^n_4Br (0.50 g, 1.6 mmol) in water (5 cm^3). Following addition of more water (*ca.* 30 cm^3) and cooling to 5 °C to complete precipitation, the crude product was collected by vacuum filtration and dried in air. Recrystallization from Pr^iOH–acetone yielded purple needles (0.60 g, 90%), m.p. 210–211 °C (Found: C, 49.5; H, 7.2; N, 2.8; S, 12.3. $C_{42}H_{72}N_2O_6PtS_4$ requires C, 49.3; H, 7.1; N, 2.7; S, 12.5%).

Preparation of dicyanomethylene-substituted complexes

$[NBu^n_4]_2[Ni(L^2)_2]$ 4. Compound **1** (0.20 g, 0.23 mmol) was dissolved with stirring in warm dmf (5 cm^3), yielding a blue solution. Malononitrile (0.05 g, 0.76 mmol) was added, and the resulting mixture stirred at *ca.* 70 °C for 10 min, during which time it became muddy green. Hot Pr^iOH (20 cm^3) was then added, and the mixture set aside to cool to room temperature. After cooling at −20 °C overnight, a mixture of greenish powder and needle crystals was collected by vacuum filtration, washed with Pr^iOH and air dried. The crude product was recrystallized by slow evaporation of a Pr^iOH–acetone mixture, yielding thick black shiny plates (0.21 g, 99%), m.p. 259–260 °C (Found: C, 57.9; H, 7.2; N, 8.7; S, 13.2. $C_{48}H_{72}N_6NiO_4S_4$ requires C, 58.6; H, 7.4; N, 8.5; S, 13.0%).

$[NBu^n_4]_2[Pd(L^2)_2]$ 5. This was prepared from complex **2** as described for the nickel analogue. Recrystallization from Pr^iOH–acetone yielded dark block-shaped crystals with purple reflex (0.19 g, 90%), m.p. 254–255 °C (Found: C, 55.8; H, 7.1; N, 7.9; S, 12.6. $C_{48}H_{72}N_6O_4PdS_4$ requires C, 55.9; H, 7.0; N, 8.1; S, 12.4%).

$[NBu^n_4]_2[Pt(L^2)_2]$ 6. This was prepared from complex **3** as described for the nickel analogue except the reaction time was 30 min. Recrystallization of the crude solids from Pr^iOH–acetone yielded fine shiny black needles (0.14 g, 67%), m.p. 265–266 °C (Found: C, 51.5; H, 6.7; N, 7.3; S, 11.6. $C_{48}H_{72}N_6O_4PtS_4$ requires C, 51.5; H, 6.5; N, 7.5; S, 11.5%).

$[NBu^n_4]_2[Pd(L^2)_2]·I_2$ 7. X-Ray-quality crystals of this compound were obtained in *ca.* 15% yield by slow interdiffusion of CH_2Cl_2 solutions containing I_2 and **5**, respectively, over a period of several weeks in a fritted H-tube (Found: C, 44.9; H, 5.7; N, 6.5; S, 10.0. $C_{48}H_{72}I_2N_6O_4PdS_4$ requires C, 44.5; H, 6.0; N, 6.4; S, 10.3%).

X-Ray crystallography

A suitable crystal of compound **7** was selected and mounted in a random orientation on a glass fibre. Rotation photographs were used to locate reflections which were then indexed to obtain the triclinic unit cell. Axial photographs confirmed the axial lengths for the unit cell. No suitable transformation could be found to a cell of higher symmetry.

Crystal data and data collection parameters. $C_{48}H_{72}I_2N_6O_4PdS_4$, $M = 1285.6$, triclinic, space group $P\bar{1}$, $a = 10.792(3)$, $b = 13.995(5)$, $c = 10.737(3)$ Å, $\alpha = 105.48(1)$, $\beta = 115.15(1)$, $\gamma = 76.51(2)°$, $U = 1401.4(5)$ $Å^3$ [by least-squares refinement on diffractometer angles from 100 centred reflections, four settings each of 25 reflections with $0.25 \leqslant (\sin\theta)/\lambda \leqslant 0.26$], $T = 294(1)$ K, $Z = 1$, $F(000) = 650$, $D_c = 1.52$ g cm^{-3}, black, rectangular block, 0.25 × 0.40 × 0.20 mm, μ(Mo-Kα) = 16.028 cm^{-1}, semiempirical absorption correction based upon ψ scans, $T_{max}/T_{min} = 1.19$; Enraf-Nonius CAD4 diffractometer, graphite-monochromated Mo-Kα radiation ($\lambda = 0.710\,69$ Å), θ–2θ scans, data collection range $2 \leqslant 2\theta \leqslant 82°$, $\pm h$, $\pm k$, $\pm l$; three standard reflections showed 6.5% average decrease in intensity during data collection, and a linear decay correction was applied. 14 830 Reflections measured, 7412 independent, averaging observed reflections yielded $R(I) = 0.017$; least-squares refinements were based on 4692 independent reflections with $F_o \geqslant 3\sigma(F_o)$.

Structure solution and refinement. All calculations were performed using the Enraf-Nonius MOLEN Package[10] on a MicroVAX 3100 computer. Neutral atom scattering factors and corrections for anomalous dispersion were taken from the usual sources.[11] The structure was solved *via* direct methods[12] and completed with Fourier-difference syntheses. Intensity statistics from the data set indicated a centrosymmetric structure. Attempts to solve the structure in space group $P\bar{1}$ were immediately successful. Weighting factors were applied to all reflections as $w = 1/\sigma(F^2)$ where $\sigma(F^2) = [\sigma(I)^2 + (pF^2)^2]^{\frac{1}{2}}$ and $p = 0.04$. All non-hydrogen atoms were refined by full-matrix least squares on F with anisotropic thermal parameters. Hydrogen atoms were located in the Fourier-difference maps, but attempts to refine all their positions led to a small number of unacceptable C–H bond lengths. The final model used calculated H-atom positions based on C–H 0.95 Å and idealized tetrahedral H–C–H angles. Hydrogen positions were updated throughout the final cycles of refinement. Final $R'(F) = 0.038$, with conventional $R(F) = 0.029$ for 295 parameters, $N_o/N_v = 15.9$, Goodness of fit = 1.223, $\Delta/\sigma = 0.01$ and $\Delta(\rho) = 0.997$ e $Å^{-3}$. Examination of strong, low-angle reflections revealed no

evidence for extinction-affected reflections. Crystal-packing interactions were analysed using SPARTAN[13] running on a Silicon Graphics Personal Iris 4D/35 workstation; Fig. 4 was drawn using the program ORTEP.[14]

Atomic coordinates, thermal parameters, and bond lengths and angles have been deposited at the Cambridge Crystallographic Data Centre (CCDC). See Instructions for Authors, *J. Chem. Soc., Dalton Trans.*, 1996, Issue 1. Any request to the CCDC for this material should quote the full literature citation and the reference number 186/160.

Results and Discussion

Synthesis

Reaction of potassium dithiocroconate (K_2L^1) with $NiCl_2 \cdot 6H_2O$ or K_2MCl_4 (M = Pd or Pt) in dmf–water solution followed by addition of NBu^n_4Br yields salts **1–3** as crystalline solids. Since reaction of K_2L^1 with K_2PtCl_4 under these conditions is slow even at elevated temperature, the platinum salt **3** is more convieniently prepared by first isolating $K_2[Pt(L^1)_2]$ from an aqueous reaction mixture and then converting it into the tetrabutylammonium salt by metathesis in dmf solution. This approach has also been used to prepare a wide range of corresponding nickel and palladium salts. By analogy with the previously reported[15] reactivity of the copper analogue, treatment of salts **1–3** with an excess of malononitrile in warm dmf solution affords dicyanomethylene-substituted derivatives **4–6** in good to excellent yields.

Spectroscopic characterization

Spectroscopic data for complexes **1–6** are summarized and compared with corresponding data for the free croconates in Table 1. The ^{13}C NMR spectrum of dithiocroconate ion (L^1) in CD_3CN solution exhibits three resonances with downfield chemical shifts indicative of the formal aromatic character[5] of this species. Complexes **1–3** likewise exhibit three ^{13}C resonances, but each peak is shifted upfield relative to its counterpart in the free L^1 spectrum. The relative magnitudes of the co-ordination-induced shifts in the resonances assigned to the C···S and C···O carbons of ligands L^1 and L^2 suggest the occurrence of M–S rather than M–O bonding in complexes **1–6**. This is consistent with S,S-chelate binding of L^1 and L^2 observed in the crystal structures of $[PPh_4]_3[Co(L^1)_3] \cdot 0.6Me_2CO$,[16] $[NBu^n_4]_2[Cu(L^2)_2]$,[15] and the iodine-inclusion compound **7** (see below).

The IR spectrum of potassium dithiocroconate shows three strong absorptions at 1660, 1609 and 1576 cm^{-1} arising from in-plane stretching vibrations of the C···O bonds, and a very strong band at 1306 cm^{-1} which is attributed to an in-plane C···S stretching vibration. Corresponding bands in the spectra of salts **1–3** are shifted to higher frequency, suggesting a modest enhancement of both the C···O and C···S bonding upon S,S co-ordination of the ligand to a metal. Comparable co-ordination-induced shifts of the strong C···S and C···O absorptions are found also for dicyanomethylene-substituted complexes **4–6**, but the CN stretching frequency is unshifted by complex formation.

The visible spectra of complexes **1–3** are compared with that of the dithiocroconate ion in Fig. 1(*a*). Free L^1 exhibits two strong, overlapping visible absorptions at 436 and 486 nm; the lower-energy band has previously been assigned[17] as π–π^* transition involving molecular orbitals with predominant C···S character. Complexes **1–3** exhibit similarly intense (ε = 15 000–25 000 $dm^3\ mol^{-1}\ cm^{-1}$) visible absorptions with λ_{max} values that are red-shifted by *ca.* 88 (M = Pd) and *ca.* 150 nm (M = Ni or Pt) relative to the corresponding bands of free L^1 (Table 1). Dicyanomethylene substitution of **1–3** to form **4–6** induces a further red-shift of *ca.* 150–225 nm in λ_{max} of the

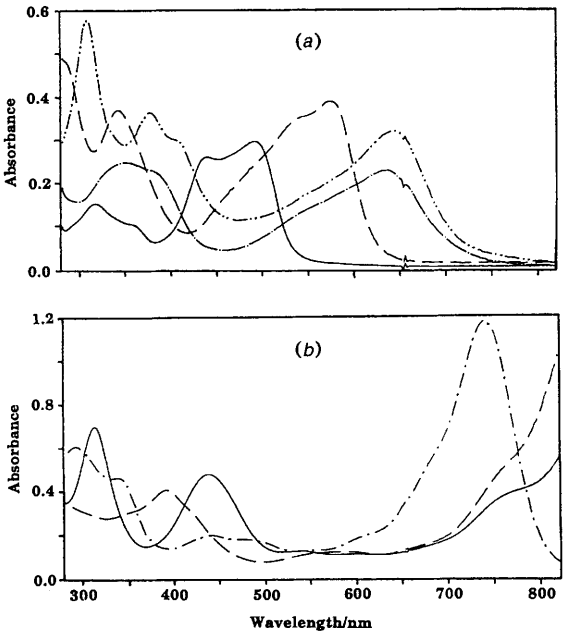

Fig. 1 Visible spectra of (*a*) compounds **1–3** compared with free L^1 [L^1 (——), **1** (- · · -), **2** (– – –), **3** (— · —)] and (*b*) dicyanomethylene-substituted analogues **4** (——), **5** (- · -) and **6** (– – –). All spectra recorded in MeCN solution and normalized to 1.5×10^{-5} mol dm^{-3} concentration

complexes and also causes a significant increase in the absorption intensity [Fig. 1(*b*), Table 1].

While intense ($\varepsilon \geqslant 15\,000$ $dm^3\ mol^{-1}\ cm^{-1}$), low-energy ($\lambda > 700$ nm) absorptions are well known for both neutral[3,18] and monoanionic[19] metal bis(dithiolenes), the observation of such absorptions in *dianionic* metal bis(dithiolene) complexes is unprecedented.* The intensity of the low-energy absorptions of **1–6** clearly indicates that they arise from symmetry-allowed electronic transitions. The pronounced metal and substituent dependence of λ_{max} for the complexes likewise implies that the transitions involve orbital(s) having both metal and ligand character. Taken together, these observations suggest that the transition responsible for the characteristic low-energy absorptions of complexes **1–6** possesses mixed intraligand and metal–ligand charge-transfer (m.l.c.t.) character.

Electrochemistry

Electrochemical data for salts **1–6** in acetonitrile solution are presented along with literature values for the corresponding $[M(mnt)_2]^{2-}$ complexes in Table 2; the effects of dicyanomethylene substitution are illustrated by comparison of the cyclic voltammograms of platinum complexes **3** and **6** in Fig. 2. Dithiocroconate complexes **1–3** each exhibit a single reversible oxidation with $E_{\frac{1}{2}}$ in the potential range 0.4–0.7 V *vs.* saturated calomel electrode (SCE). While the oxidation potentials of **1–3** are *ca.* 200 mV more positive than those of their $[M(mnt)_2]^{2-}$ analogues, the metal dependence of the oxidation potential nonetheless follows the same trend: Ni ≈ Pt < Pd. The oxidation potentials of dicyanomethylene-substituted analogues **4–6** vary similarly, but in this case the oxidation is irreversible due to formation of a film on the surface of the working electrode. More importantly, dicyanomethylene substitution of the ligands in **4–6** causes a further anodic shift of *ca.* 100–200 mV relative to the $E_{\frac{1}{2}}$ values recorded for **1–3**. Based

* For comparison, corresponding low-energy charge-transfer bands in solution spectra of the $[M(mnt)_2]^{2-}$ (M = Ni, Pd or Pt; mnt = maleonitriledithiolate) analogues fall between 470 and 525 nm with $\varepsilon \leqslant 6000$ $dm^3\ mol^{-1}\ cm^{-1}$.[1a]

Table 1 Spectroscopic data

Compound	IR[a]/cm^{-1}		^{13}C NMR (δ)[b]					UV/VIS[c]
	ν(C=O)	ν(C–S)	1	2	3	4	5	λ_{max}/nm (log ε)
1	1690, 1671, 1641	1398	191.4	191.0	182.4			640 (4.32)
2	1692, 1671, 1644	1408	190.3	189.4	184.1			574 (4.41)
3	1686, 1671, 1642	1395	190.9	186.5	184.5			636 (4.18)
K_2L^1	1660, 1609, 1576	1306[d]	205.3	187.4	186.5			486 (4.29)
4	1686, 1651, 1628	1404	189.3	177.6	155.8	71.8	114.0	867 (≥4.6)
5	1689, 1650, 1631	1406	188.6	178.9	154.5	72.2	113.9	740 (4.89)
6	1685, 1653, 1630	1400	185.4	180.0	155.8	74.0	113.8	843 (≥4.8)
K_2L^2	1660, 1580	1315[d,e]	199.4	187.5	146.2	56.7	117.9[f]	571[g]

[a] In CH_2Cl_2 solution. [b] Chemical shifts relative to $SiMe_4$ in CD_3CN solution unless otherwise noted. Peak 1 is the C$^{\cdot\cdot}$S carbon, 5 the CN carbon, and 2–4 are assigned to intervening carbons in order of increasing distance from the C$^{\cdot\cdot}$S carbons. [c] In MeCN solution unless otherwise noted. [d] As KBr mull. [e] Ref. 8. [f] In D_2O. [g] In water.

Table 2 Electrochemical data[a]

M	Couple	Ligand		
		L^1	L^2	mnt
Ni	−1/−2	0.47	0.66[b]	0.23[c]
	−2/−3	−1.26	−0.70	−1.67[d]
	−3/−4	−1.44[e]	−0.94	n.o.
Pd	−1/−2	0.66	0.74[b]	0.46[c]
	−2/−3	−1.26[e]	−0.66	−1.90[d]
	−3/−4	−1.5[f]	−0.85	n.o.
Pt	−1/−2	0.40	0.58[b]	0.21[c]
	−2/−3	−1.30	−0.69	−2.22[d]
	−3/−4	−1.50	−0.94	−2.44[d]

[a] $E_{\frac{1}{2}}$ in volts *vs.* SCE, MeCN, 0.10 mol dm^{-3} electrolyte; n.o. = not observed. [b] Irreversible, E_{pa}. [c] Ref. 1(*a*). [d] Ref. 20. [e] Quasi-reversible. [f] Irreversible, E_{pc}.

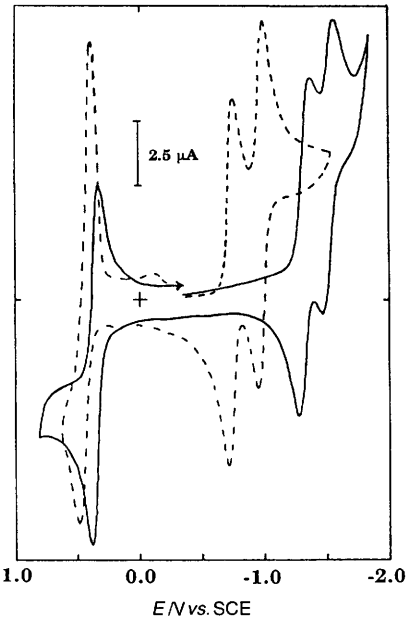

Fig. 2 Cyclic voltammograms of compounds **3** (——) and **6** (– – – –) in MeCN solution, 0.1 mol dm^{-3} [NBu^n_4][BF_4], sweep rate = 200 mV s^{-1}

on comparision of $E_{\frac{1}{2}}$ values, complexes **1–6** exhibit greater resistance to oxidation than do any previously reported metal bis(dithiolene) complexes.

Cathodic scans of complexes **1–3** reveal in each case a pair of closely spaced ($\Delta E_{\frac{1}{2}}$ *ca.* 200–250 mV) reversible or quasi-reversible one-electron reduction waves with $E_{\frac{1}{2}}$ values between −1.25 and −1.50 V *vs.* SCE; in contrast to the metal dependence of the oxidation waves, the $E_{\frac{1}{2}}$ values for the reduction processes are essentially independent of the metal ion. As clearly illustrated in Fig. 2, dicyanomethylene substitution of the ligand exerts a considerably greater influence upon the reductive electrochemistry of the complexes than that seen in the case of the oxidations. Like the parent complexes **1–3**, the dicyanomethylene-substituted derivatives **4–6** each exhibit two reversible reduction waves, separated by *ca.* 200–250 mV, with $E_{\frac{1}{2}}$ values that are essentially independent of the metal ion. However, introduction of the more electronegative dicyanomethylene substituent on the ligand periphery induces a very large (*ca.* 500–650 mV) anodic shift in the reduction potentials of **4–6** relative to the corresponding potentials of **1–3**.

ESR spectra of oxidized and reduced complexes

Owing to the apparent instability of the one-electron oxidation products, attempts to isolate analytically pure samples of monoanion salts of these complexes have thus far proven unsuccessful. However, oxidation of the nickel complexes **1** and **4** with I_2 in MeCN solution at 25 °C, followed by rapid quenching at 77 K, yielded samples exhibiting clean rhombic ESR spectra similar to that reported[21] for the well characterized $[Ni(mnt)_2]^-$ ion. The observed *g*-tensor components (Table 3) have been assigned by analogy with those determined[21b] for $[Ni(mnt)_2]^-$ in magnetically dilute single crystals, namely: $g_1 = g_x$, $g_2 = g_y$ and $g_3 = g_z$, where g_1 and g_3 refer to the lowest- and highest-field *g* values. Low-temperature

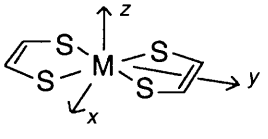

(−20 °C) galvanostatic electrolysis of MeCN solutions containing the palladium and platinum salts **2**, **3**, **5** and **6** likewise produced radicals exhibiting ESR spectra (Table 3, Fig. 3) that are remarkably similar to those of the corresponding $[M(mnt)_2]^-$ analogues.

Bulk galvanostatic electroreduction of complexes **1–6** in Ar-saturated CH_2Cl_2 and MeCN solutions at both ambient and low temperature produced highly air-sensitive radicals exhibiting relatively narrow ($\Delta H_{p\text{-}p}$ = 5–30 G) ESR signals centred near g = 2.00 in frozen solution at 77 K. However, the appearance of the spectra was found to depend strongly upon the electrolysis conditions, and evidence of decomposition was noted in the UV/VIS spectra of some of the solutions. Thus, it remains unclear whether the signals observed arise from the intact reduced complexes or some decomposition product.

Crystal structure of compound 7

Crystals of compound **7** are triclinic, space group $P\bar{1}$. The Pd atom sits on the inversion centre. The centrosymmetric complex anions are linked together by S···I–I···S bridges to form

Table 3 The ESR data[a]

		L^1			L^2			mnt		
M		x	y	z	x	y	z	x	y	z
Ni	g	2.137	2.047	2.003	2.123	2.044	2.000	2.140	2.042	1.998[b]
Pd	g	2.046[c]		1.968	2.042[c]		1.974	2.065	2.056	1.956[b]
Pt	g	2.256	2.052	1.832	2.248	2.049	1.836	2.221	2.067	1.825[d]
	A^{Pt}	⩽60[e]	336	249	⩽60[e]	407	249	0 (±3)	376	297

[a] Spectra recorded in low temperature (77 K) solvent glass unless otherwise noted. The g-tensor components have been assigned by analogy with those determined by single-crystal measurements [refs. 21(*b*) and 22]. Hyperfine parameters are given in MHz. [b] Ref. 21(*a*). [c] The x and y components are not resolved. [d] Single-crystal g values and ^{195}Pt hyperfine splittings from ref. 22. [e] Upper limit based upon measured half-width at half-height of x component = 20 G.

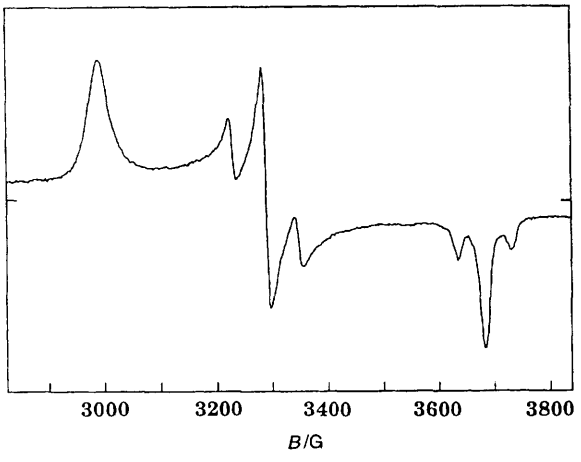

Fig. 3 Low-temperature (77 K) ESR spectrum of $[Pt(L^1)_2]^-$ ion formed by electrooxidation of compound **3**. Acetonitrile solution 0.1 mol dm^{-3} $[NBu^n_4][BF_4]$, microwave frequency 9.4623 GHz

stair-like 'chains' extending along [100], with the bond axis of the I_2 molecule inclined at an angle of 74° relative to the PdS_4 plane. The observed S···I distance [3.1696(9) Å] is considerably shorter than the sum of the van der Waals radii (4.00 Å) for these atoms,[23] but the I–I bond length [2.7354(4) Å] is comparable to the value [2.715(6) Å] found[24] in solid I_2, indicating that the degree of intermolecular charge transfer associated with the S···I interaction is small.

An ORTEP plot of the $[Pd(L^2)_2]^{2-}$ anion in the structure is presented in Fig. 4. The small but significant difference in the length of the two independent Pd–S bonds (Table 4) presumably results from the exclusive interaction of the I_2 molecule with S(2). The Pd–S distances in the present structure are both slightly longer than the average values [2.292(4) and 2.278(5) Å] found[25] for the $[Pd(mnt)_2]^-$ monoanion in its hydrated K^+ and NH_4^+ salts, respectively; this is consistent with the antibonding character of the M–L interaction in the $2b_{3g}$ HOMO (highest occupied molecular orbital) of the present complexes (see below). The mean plane defined by the ligand atoms is inclined by *ca.* 4° relative to the planar PdS_4 core, giving the centrosymmetric complex as a whole a slight 'chair' conformation. Examination of the crystal packing suggests that this distortion results from close intermolecular contacts between pairs of overlapping $C(CN)_2$ groups on neighbouring anions along [010]. The CO and CN groups of each ligand are also displaced slightly from the mean plane defined by the remaining ligand atoms, resulting in a staggered conformation for these groups when viewed down the axis of the peripheral C=C bond; this distortion likewise appears to be a consequence of close anion–cation contacts within the structure.

The electron structure of complexes 1–6

The results of a number of electronic structure calculations on nickel bis(dithiolene) complexes have been summarized by

Table 4 Selected bond distances (Å) and angles (°) for compound **7**

I–I	2.7354(4)	C(1)–C(2)	1.382(3)
Pd–S(1)	2.3101(9)	C(1)–C(5)	1.471(5)
Pd–S(2)	2.3014(7)	C(2)–C(3)	1.456(4)
S(1)–C(1)	1.690(3)	C(3)–C(4)	1.487(4)
S(2)–C(2)	1.705(3)	C(4)–C(5)	1.475(3)
O(1)–C(3)	1.221(3)	C(4)–C(6)	1.350(5)
O(2)–C(5)	1.219(3)	C(6)–C(7)	1.432(3)
N(1)–C(7)	1.143(4)	C(6)–C(8)	1.437(5)
N(2)–C(8)	1.147(5)		
S(1)–Pd–S(1)	180.0(0)	O(1)–C(3)–C(4)	125.9(3)
S(1)–Pd–S(2)	90.30(3)[a]	O(1)–C(3)–C(2)	128.1(3)
S(1)–Pd–S(2)	89.70(3)[b]	C(3)–C(4)–C(5)	107.6(2)
S(2)–Pd–S(2)	180.0(0)	C(3)–C(4)–C(6)	125.5(2)
Pd–S(1)–C(1)	101.0(1)	C(5)–C(4)–C(6)	126.9(2)
Pd–S(2)–C(2)	101.06(8)	C(1)–C(5)–C(4)	106.1(2)
S(1)–C(1)–C(2)	124.1(3)	O(2)–C(5)–C(1)	127.9(3)
S(1)–C(1)–C(5)	126.2(2)	O(2)–C(5)–C(4)	126.0(3)
C(2)–C(1)–C(5)	109.7(2)	C(4)–C(6)–C(7)	122.7(3)
C(1)–C(2)–C(3)	110.5(3)	C(4)–C(6)–C(8)	123.5(2)
S(2)–C(2)–C(3)	125.8(2)	C(7)–C(6)–C(8)	113.8(3)
S(2)–C(2)–C(1)	123.5(2)	N(1)–C(7)–C(6)	176.0(3)
C(2)–C(3)–C(4)	105.9(2)	N(2)–C(8)–C(6)	175.3(4)

[a] Intraligand angle. [b] Interligand angle.

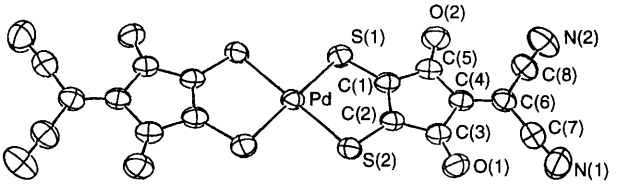

Fig. 4 An ORTEP plot of $[Pd(L^2)_2]^{2-}$ ion in compound **7**

Alvarez *et al.*[26] The relevant molecular orbitals may be represented in the form of a qualitative energy-level diagram as shown in Fig. 5. The HOMO of the (formally) d^8 nickel mono- and di-anion complexes is the $2b_{3g}$ orbital, which has mixed metal–ligand character.* Discrete variational Xα calculations performed on the $[Ni(mnt)_2]^z$ ($z = -1$ or -2) ions indicate[27] that this orbital has predominant (*ca.* 60%) ligand S(3p) character and a smaller (*ca.* 20–30%) contribution from the $Ni(3d_{yz})$ orbital, a result consistent with the three-fold g anisotropy and hyperfine splittings observed in the ESR spectra of paramagnetic ($S = \frac{1}{2}$) $[M(mnt)_2]^-$ (M = Ni, Pd or Pt) ions.[21,22] Since the ESR parameters observed for the paramagnetic monoanions obtained by oxidation of **1–6** are

* Several previous papers have employed a coordinate system in which the x and y axes are transposed relative to that shown in Fig. 5, leading to symmetry label b_{2g} rather than b_{3g} for this orbital; for consistency, we have assigned orbital symmetry labels using the same coordinate system previously used to assign the g-tensor components in single-crystal ESR studies.[21b,22]

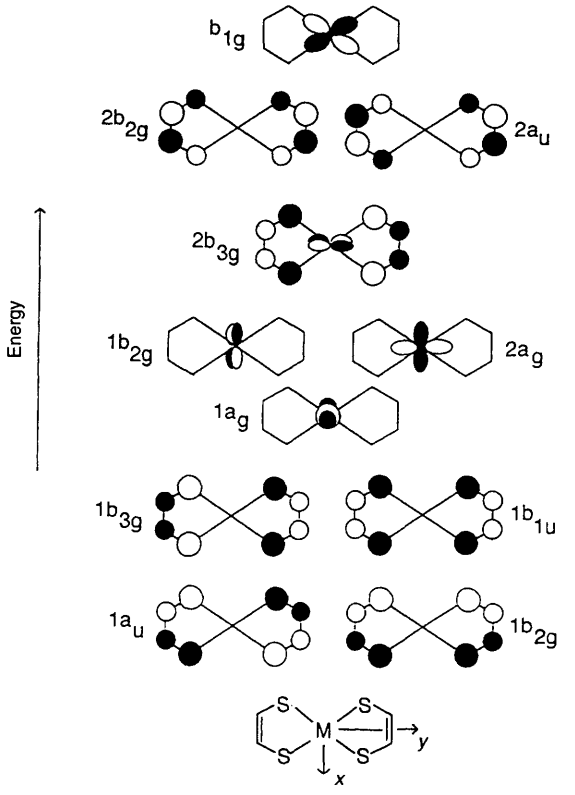

Fig. 5 Molecular orbitals for $M(dithiolene)_2$ complexes (after ref. 26)

remarkably similar to those of the latter complexes (Table 3), we conclude that complexes **1–6** also possess a similar $2b_{3g}$ HOMO.

While assignment of the $2b_{3g}$ HOMO in these complexes appears to be quite definitive, the distribution of the neighbouring valence orbitals is less certain. In particular, the level order of the $2b_{2g}$, $2a_u$, and b_{1g} orbitals lying immediately above the $2b_{3g}$ HOMO (Fig. 5) varies from one calculation to another, and in several cases was noted[26,28] to depend sensitively upon the parametrization. Experimental evidence likewise indicates that the energy ordering of these orbitals can be influenced by the metal ion. For example, while single-crystal optical studies of the $[M(mnt)_2]^{2-}$ (M = Ni or Pd) ions led to assignment[29] of a metal-based $b_{1g}(d_{xy})$ LUMO (lowest unoccupied molecular orbital) for these complexes, corresponding studies of the $[Pt(mnt)_2]^{2-}$ ion suggested[30] a ligand-based $a_u(\pi^*)$ LUMO. The different orbital character of the $[Pt(mnt)_2]^{2-}$ LUMO is also evident in the reductive electrochemistry of the $[M(mnt)_2]^{2-}$ (M = Ni, Pd or Pt) complexes. The complexes of Ni and Pd each undergo single, reversible reductions to the air-sensitive, but otherwise stable trianions, ESR spectra of which are indicative of $^2B_{1g}(d_{xy})$ ground states.[20] In contrast, the $[Pt(mnt)_2]^{2-}$ ion exhibits two closely spaced, one-electron reduction waves, but the spectroscopic properties of the presumed ligand-reduced species could not be further characterized owing to their instability and/or reactivity.[20] In view of the strong similarity between the reductive electrochemistry of complexes **1–6** and that of the $[Pt(mnt)_2]^{2-}$ ion, we propose that **1–6** also possess LUMOs with predominant ligand π^* character.

Trends in the metal and substituent dependences of the observed redox potentials for complexes **1–6** are consistent with the proposed $2b_{3g}$ HOMO and ligand π^* LUMO assignments. Thus, while the oxidation potentials within each series (*i.e.* **1–3** and **4–6**) exhibit a pronounced metal dependence, as would be expected for removal of an electron from a $2b_{3g}$ HOMO having significant metal character, the corresponding reduction potentials are essentially metal independent, indicating that reduction involves transfer of electrons into a predominantly ligand-based LUMO. Similarly, while replacing the central oxo-groups of each ligand with more strongly electron-withdrawing[31] dicyanomethylene groups induces significant anodic shifts in both the oxidation and reduction potentials, the magnitude of the shift is *ca.* 2–3 times larger for the ligand-based reductions than for the oxidations.

It is of interest to consider the origin of the intense, low-energy absorptions of complexes **1–6**. If the LUMO is assumed to be the $2a_u(\pi^*)$ orbital shown in Fig. 5, then the intense visible absorptions of **1–6** may be reasonably attributed to the symmetry-allowed $2b_{3g}(\pi,d_{yz}) \longrightarrow 2a_u(\pi^*)$ transition. This transition is quite different from that responsible for the intense, near-IR absorptions of the neutral and monoanionic nickel bis(dithiolene) complexes noted previously. Since the latter complexes have a vacancy in the $2b_{3g}$ HOMO, they can exhibit low-energy absorption arising from the symmetry-allowed $1b_{1u}(\pi) \longrightarrow 2b_{3g}(\pi,d_{yz})$ transition.[28] Interest in such complexes as Q-switching laser dyes arises from the observation[3] that this absorption can be red-shifted into the near-IR region by π-donor substituents, an effect which has been attributed[3,28] to the preferential destabilization of the ligand-based $1b_{1u}(\pi)$ orbital by the electron-donating substituents. However, it has also previously been noted[3] that the use of electron-donating substituents can have the undesirable effect of decreasing the oxidative stability of the chromophore.

The relatively low energy and marked substituent dependence of the proposed $2b_{3g}(\pi,d_{yz}) \longrightarrow 2a_u(\pi^*)$ transition in the dianionic metal bis(dithiolenes) **1–6** can be accounted for in a manner completely analogous to that just described for the neutral and monoanionic analogues. In this case the electron-withdrawing substituents are expected preferentially to stabilize the ligand-based $2a_u(\pi^*)$ LUMO relative to the $2b_{3g}$ HOMO, but the net result is the same: a decrease in the HOMO – LUMO energy gap and a red-shift in the visible λ_{max} of the complexes. The substantially lower transition energies observed for the dicyanomethylene-substituted complexes **4–6** are in accord with the stronger π-acceptor character of the $=C(CN)_2$ group relative to the oxo group.[31] More importantly, the use of strongly electron-withdrawing substituents to shift the absorbance in this case has the beneficial effect of increasing, rather than decreasing, the apparent oxidative stability of the complexes.

Conclusion

The results presented in this paper provide the first demonstration that stabilization of the ligand-based $2a_u(\pi^*)$ orbital by strongly electron-withdrawing ligand substituents provides an effective means of promoting intense, low-energy absorption in dianionic metal bis(dithiolene) complexes. This alternative approach to the preparation of near-IR absorbing metal bis(dithiolene) complexes shows particular promise, because the introduction of electron-withdrawing substituents increases, rather than decreases, the oxidative stability of the complexes. Efforts are currently under way to prepare metal bis(dithiocroconate) complexes bearing greater numbers of dicyanomethylene substituents, since such complexes are expected to exhibit even more favourable spectroscopic and electrochemical properties. The non-linear optical properties of complexes **1–6** are also being investigated, and will be described separately.

Acknowledgements

Support of this work by the Naval Academy Research Council is gratefully acknowledged. We also thank Mr. Kysler M. De Guzman of Bowling Green State University for measurement of NIR spectra.

References

1 (*a*) J. A. McCleverty, *Prog. Inorg. Chem.*, 1968, **10**, 49; (*b*) R. P. Burns and C. A. McAulliffe, *Adv. Inorg. Chem. Radiochem.*, 1979, **22**, 303; (*c*) U. T. Mueller-Westerhoff and B. Vance, in *Comprehensive Coordination Chemistry*, ed. G. Wilkinson, Pergamon, Oxford, 1987, vol. 2, pp. 595–631.

2 P. Cassoux, L. Valade, H. Kobayashi, A. Kobayashi, R. A. Clark and A. E. Underhill, *Coord. Chem. Rev.*, 1991, **110**, 115; J. S. Miller and A. J. Epstein, *Angew. Chem., Int. Ed. Engl.*, 1994, **33**, 385.

3 U. T. Mueller-Westerhoff, B. Vance and D. I. Yoon, *Tetrahedron*, 1991, **47**, 909.

4 G. Seitz, K. Mann and R. Matusch, *Arch. Pharm. (Weinheim, Ger.)*, 1975, **308**, 792.

5 R. West and J. Niu, in *Nonbenzenoid Aromatics*, ed. J. P. Snyder, Academic Press, New York, 1969, vol. 1, ch. 6, pp. 311–345.

6 R. West and H. Y. Niu, *J. Am. Chem. Soc.*, 1963, **85**, 2586; D. Deguenon, G. Bernardinelli, J.-P. Tuchagues and P. Castan, *Inorg. Chem.*, 1990, **29**, 3031; I. Castro, J. Sletten, J. Faus, M. Julve, Y. Journaux, F. Lloret and S. Alvarez, *Inorg. Chem.*, 1992, **31**, 1889.

7 (*a*) R. F. X. Williams, *Phosphorus Sulfur Relat. Elem.*, 1976, **2**, 141; (*b*) P. S. Santos, *J. Mol. Struct.*, 1990, **220**, 137.

8 G. Arndt, T. Kampchen, R. Schmiedel, G. Seitz and R. Sutrisno, *Liebigs Ann. Chem.*, 1980, 1409.

9 G. Gritzner and J. Kuta, *Pure Appl. Chem.*, 1984, **56**, 461.

10 MOLEN, An Interactive Structure Solution Procedure, Enraf-Nonius, Delft, 1990.

11 *International Tables for X-Ray Crystallography*, eds. J. A. Ibers and W. C. Hamilton, Kynoch Press, Birmingham, 1974, vol. 4.

12 P. Main, S. J. Fiske, S. E. Hull, L. Lessinger, G. Germain, J. P. DeClerq and M. M. Woolfson, MULTAN 11/82, A System of Computer Programs for the Automatic Solution of Crystal Structures from X-Ray Diffraction Data, University of York, 1982.

13 SPARTAN 3.1, Electronic Structure Program, Wavefunction, Inc., Irvine, CA, 1991.

14 C. K. Johnson, ORTEP II, A Fortran Thermal Ellipsoid Plot Program for Crystal Structure Illustrations, Report ORNL-5138, Oak Ridge National Laboratory, Oak Ridge, TN, 1976.

15 N. Venkatalakshmi, B. Varghese, S. Lalitha, R. F. X. Williams and P. T. Manoharan, *J. Am. Chem. Soc.*, 1989, **111**, 5748.

16 W. B. Heuer and W. H. Pearson, *Polyhedron*, 1996, **15**, 2199.

17 P. S. Santos, *J. Mol. Struct.*, 1990, **216**, 1.

18 F. Bigoli, P. Deplano, F. A. Devillanova, V. Lippolis, P. J. Lukes, M. L. Mercuri, M. A. Pellinghelli and E. F. Trogu, *J. Chem. Soc., Chem. Commun.*, 1995, 371; C. A. S. Hill, A. Charlton, A. E. Underhill, K. M. A. Malik, M. B. Hursthouse, A. I. Karaulov, S. N. Oliver and S. V. Kershaw, *J. Chem. Soc., Dalton Trans.*, 1995, 587.

19 I. Hawkins and A. E. Underhill, *J. Chem. Soc., Chem. Commun.*, 1990, 1593; S. B. Wilkes, I. R. Butler, A. E. Underhill, M. B. Hursthouse, D. E. Hibbs and K. M. A. Malik, *J. Chem. Soc., Dalton Trans.*, 1995, 897; A. Charlton, A. E. Underhill, A. Kobayashi and H. Kobayashi, *J. Chem. Soc., Dalton Trans.*, 1995, 1285.

20 W. E. Geiger, jun., C. S. Allen, T. E. Mines and F. C. Senftleber, *Inorg. Chem.*, 1977, **16**, 2003.

21 (*a*) A. Davison, N. Edelstein, R. H. Holm and A. H. Maki, *J. Am. Chem. Soc.*, 1963, **85**, 2029; (*b*) A. H. Maki, N. Edelstein, A. Davison and R. H. Holm, *J. Am. Chem. Soc.*, 1964, **86**, 4580.

22 R. Kirmse, W. Dietzsch and B. V. Solov'ev, *J. Inorg. Nucl. Chem.*, 1977, **39**, 1157.

23 L. Pauling, *The Nature of the Chemical Bond*, 3rd edn., Cornell University Press, Ithaca, NY, 1960, ch. 7, p. 260.

24 F. van Bolhuis, P. B. Koster and T. Migchelsen, *Acta Crystallogr.*, 1967, **23**, 90.

25 M. B. Hursthouse, R. L. Short, P. I. Clemenson and A. E. Underhill, *J. Chem. Soc., Dalton Trans.*, 1989, 67.

26 S. Alvarez, R. Vicente and R. Hoffmann, *J. Am. Chem. Soc.*, 1985, **107**, 6253.

27 M. Sano, H. Adachi and H. Yamatera, *Bull. Chem. Soc. Jpn.*, 1981, **54**, 2636.

28 Z. S. Herman, R. F. Kirchner, G. H. Loew, U. T. Mueller-Westerhoff, A. Nazzal and M. C. Zerner, *Inorg. Chem.*, 1982, **21**, 46.

29 G. V. R. Chandramouli and P. T. Manoharan, *Inorg. Chem.*, 1986, **25**, 4680; W. Guntner, G. Gliemann, H. Kunkely, C. Reber and J. I. Zink, *Inorg. Chem.*, 1990, **29**, 5238.

30 W. Guntner and G. Gliemann, *J. Phys. Chem.*, 1990, **94**, 618.

31 K. Wallenfels, K. Friedrich, J. Rieser, W. Ertel and H. K. Thieme, *Angew. Chem., Int. Ed. Engl.*, 1976, **15**, 261.

Received 26*th January* 1996; *Paper* 6/00608F